N89-22951

CALCULATION OF LOW FREQUENCY VIBRATIONAL RESONANCES OF SUBMERGED STRUCTURES

by

Gordon C. Everstine

Applied Mathematics Division (184)
David Taylor Research Center
Bethesda, Maryland 20084 U.S.A.

ABSTRACT

Numerical techniques for calculating the low frequency vibrational resonances of submerged structures are reviewed. Both finite element and boundary element approaches for calculating fully-coupled added mass matrices for use in NASTRAN analysis are described and illustrated. The finite element approach is implemented using existing capability in NASTRAN. The boundary element approach uses the NASHUA structural-acoustics program to compute the added mass matrix. The two procedures are compared to each other for the case of a submerged cylindrical shell with flat end closures. It is concluded that both procedures are capable of computing accurate submerged resonances and that the more elegant boundary element procedure is easier to use but may be more expensive computationally.

INTRODUCTION

One problem of interest in numerical structural-acoustics is that of determining the natural vibrational frequencies of general submerged structures. At low frequencies, it is known[1] that the fluid appears to the structure like an added mass (i.e., the fluid pressure on the wet surface is in phase with structural acceleration). At higher frequencies, the fluid impedance (the ratio of fluid pressure to velocity) is mathematically complex, since it involves both mass-like and damping-like effects. The primary difference between these two situations from a computational point of view is that the low frequency calculation can be performed using standard real eigenvalue analysis techniques, whereas the higher frequency calculation requires more expensive complex eigenanalysis. In addition, as frequency increases, the added mass effects decline and the damping (or piston) effects increase, so that the interpretation of the complex eigenvectors as "normal modes" becomes more difficult. For shell structures, such complications become somewhat academic, since shells have high modal density above the first few modes, making the usefulness of computing such modes in doubt anyway.

Consequently, for this paper, we restrict our interest to the calculation of low frequency modes, in which case the finite element calculation of

submerged resonances reduces to that of computing the added mass effects of the surrounding fluid on the structure. The added mass calculation requires solving Laplace's equation in the fluid domain exterior to the structure, a calculation which can be performed using either finite element or boundary element techniques, among others. Here we describe the NASTRAN computation of submerged natural frequencies using both approaches. We start by summarizing the relevant theory and then illustrate the two approaches using as an example the vibrations of a submerged cylindrical shell with flat end closures.

THEORETICAL APPROACHES

Consider an arbitrary three-dimensional elastic structure submerged in a heavy fluid like water. The structure is modeled mathematically using the equations of elasticity and the engineering approximations for beams, plates, and shells. A finite element model of a free, undamped structure yields the matrix equation

$$M\ddot{u} + Ku = 0, \tag{1}$$

where M and K are the structural mass and stiffness matrices, respectively, and u is the vector of displacement components. The fluid is modeled mathematically as a medium for which the pressure satisfies (in the time domain) the scalar wave equation[2,3]

$$\nabla^2 p = \ddot{p}/c^2, \tag{2}$$

where c is the speed of sound in the fluid. At the fluid-structure interface, momentum and continuity considerations require that the fluid pressure be applied to the structure and that the normal derivative of pressure be proportional to normal acceleration:

$$\partial p/\partial n = -\rho \ddot{u}_n, \tag{3}$$

where n is the outward normal (from the structure into the fluid) at the interface, and ρ is the mass density of the fluid. We consider two numerical approaches to treating the fluid domain: finite element and boundary element.

Finite Element Approach

Since the scalar wave equation (2) is a special case of the vector wave equation satisfied by the structural displacements, the fluid domain can be modeled using the same types of elastic finite elements used to model the structure if an analogy is drawn between structural displacement and fluid

pressure.[4] Thus, if finite elements are used to model both structure and fluid, the system of coupled equations which results is of the form

$$\begin{bmatrix} M & 0 \\ -\rho L^T & Q \end{bmatrix} \begin{Bmatrix} \ddot{u} \\ \ddot{p} \end{Bmatrix} + \begin{bmatrix} 0 & 0 \\ 0 & C \end{bmatrix} \begin{Bmatrix} \dot{u} \\ \dot{p} \end{Bmatrix} + \begin{bmatrix} K & L \\ 0 & H \end{bmatrix} \begin{Bmatrix} u \\ p \end{Bmatrix} = \begin{Bmatrix} 0 \\ 0 \end{Bmatrix}, \tag{4}$$

where p is the vector of fluid pressures at the fluid grid points, Q and H are the fluid counterparts to the structural mass and stiffness matrices, respectively, -L is the rectangular area matrix which converts a vector of fluid pressures (positive in compression) at the wet structural points to a vector of forces at all points in the output coordinate systems selected by the user, and C is a radiation boundary condition matrix with nonzero entries only for fluid DOF on the outer boundary. (Radiation boundary conditions are intended to transmit, rather than reflect, outgoing waves.) A useful alternative to the nonsymmetric system, Eq. 4, is the symmetric potential formulation,[3] which is obtained by transforming from fluid pressure p to fluid velocity potential q (the time integral of pressure) as the fundamental fluid unknown:

$$\begin{bmatrix} M & 0 \\ 0 & Q \end{bmatrix} \begin{Bmatrix} \ddot{u} \\ \ddot{q} \end{Bmatrix} + \begin{bmatrix} 0 & L \\ L^T & C \end{bmatrix} \begin{Bmatrix} \dot{u} \\ \dot{q} \end{Bmatrix} + \begin{bmatrix} K & 0 \\ 0 & H \end{bmatrix} \begin{Bmatrix} u \\ q \end{Bmatrix} = \begin{Bmatrix} 0 \\ 0 \end{Bmatrix}. \tag{5}$$

To model the fluid with standard elastic finite elements, we let the z-component of displacement represent the velocity potential q, fix all other DOF at fluid grid points, and specify the fluid element elastic properties as[2]

$$G_e = -1/\rho, \quad E_e = -10^{20}/\rho, \quad \nu_e = \text{unspecified}, \tag{6}$$

where the subscript "e" is added to emphasize that these are the values entered on input data cards (e.g., MAT1 in NASTRAN) for the elements. Under the analogy, the element "mass density" ρ_e specified for the fluid is

$$\rho_e = \begin{cases} 0, & \text{incompressible fluid } (c \to \infty) \\ -1/(\rho c^2), & \text{compressible fluid (c finite).} \end{cases} \tag{7}$$

This specification of material properties is required for symmetry of the coefficient matrices in Eq. 5.

For large expanses of exterior fluid, only a small portion of fluid need be modeled.[5,6] For an incompressible fluid, the outer boundary may be located

at one or two structural diameters away from the structure and a pressure-release (p=0) boundary condition imposed (with SPCs). For a compressible fluid, the outer boundary is located at one or two acoustic wavelengths away from the structure, and dashpots of constant $-A/(\rho c)$ are attached between the fluid DOF and ground to absorb (approximately) the outgoing waves. (This is the plane-wave absorbing boundary condition.)

The above theoretical description allows for the possibility of fluid compressibility effects, which impose requirements on the fluid mesh size and extent and require complex eigenanalysis for the solution of Eq. 4. Since often the interest is in low frequency vibrations, which is equivalent to assuming fluid incompressibility, we specialize the above equations to the case $c \to \infty$. For an incompressible fluid, the matrices Q and C above vanish, and the coupled system (4) simplifies to

$$\begin{bmatrix} M & 0 \\ -\rho L^T & 0 \end{bmatrix} \begin{Bmatrix} \ddot{u} \\ \ddot{p} \end{Bmatrix} + \begin{bmatrix} K & L \\ 0 & H \end{bmatrix} \begin{Bmatrix} u \\ p \end{Bmatrix} = \begin{Bmatrix} 0 \\ 0 \end{Bmatrix}. \tag{8}$$

An alternative form of Eq. 8 results if the pressure vector p is eliminated from this system to yield

$$(M + M_a)\, \ddot{u} + K\, u = 0, \tag{9}$$

where the symmetric, non-banded matrix $M_a = \rho L H^{-1} L^T$ is referred to as the added mass matrix.

The low frequency (added mass) vibration problem can be solved using the symmetric potential formulation (Eq. 5 with Q and C both zero), the pressure formulation (Eq. 8), or the added mass matrix formulation (Eq. 9). The last form, Eq. 9, has the advantage of being in standard form for a real eigenvalue problem and, moreover, allows the added mass matrix to be calculated using any suitable approach, including boundary elements and finite elements. However, Eq. 9 has the (considerable) disadvantage that matrix bandedness is destroyed, since M_a couples all the wet DOF to each other. If the surrounding fluid domain is modeled with finite elements, the eigenvalue problem can alternatively be solved using Eqs. 5 or 8, which have more DOF than Eq. 9 but remain banded (if the structural and fluid unknowns are properly sequenced). The main distinction between Eqs. 5 and 8 is that the latter involves nonsymmetric coefficient matrices. Although Eq. 8 is a real eigenvalue problem, it can not be solved as such by NASTRAN (because of the nonsymmetry) and must be solved using complex eigenvalue analysis.

Boundary Element Approach

The added mass matrix in Eq. 9 can also be obtained by boundary element techniques.[7-11] In the frequency domain, where the time dependence $\exp(i\omega t)$ is suppressed, the basis for such an approach is the Helmholtz surface integral equation satisfied by the fluid pressure p on the surface S of a submerged structure:

$$\int_S p(\underline{x})(\partial D(r)/\partial n)dS - \int_S q(\underline{x})D(r)dS = p(x')/2, \quad x' \text{ on } S \tag{10}$$

where D is the Green's function

$$D(r) = e^{-ikr}/4\pi r, \tag{11}$$

$$q = \partial p/\partial n = -i\omega\rho v_n, \tag{12}$$

$k = \omega/c$ is the acoustic wave number, c is the speed of sound in the fluid, r is the distance from $\underline{x}$ to $\underline{x}'$ (Fig. 1), ρ is the mass density of the fluid, and v_n is the outward normal component of velocity on S. As shown in Fig. 1, $\underline{x}$ and $\underline{x}'$ in Eq. 4 are the position vectors for points P_j and P_i on the surface S, the vector $\underline{r} = \underline{x}' - \underline{x}$, and $\underline{n}$ is the unit outward normal at P_j. We denote the lengths of the vectors $\underline{x}$, $\underline{x}'$, and $\underline{r}$ by x, x', and r, respectively. The normal derivative of the Green's function D appearing in Eq. 10 can be evaluated as

$$\partial D(r)/\partial n = (e^{-ikr}/4\pi r)\ (ik + 1/r)\cos\beta, \tag{13}$$

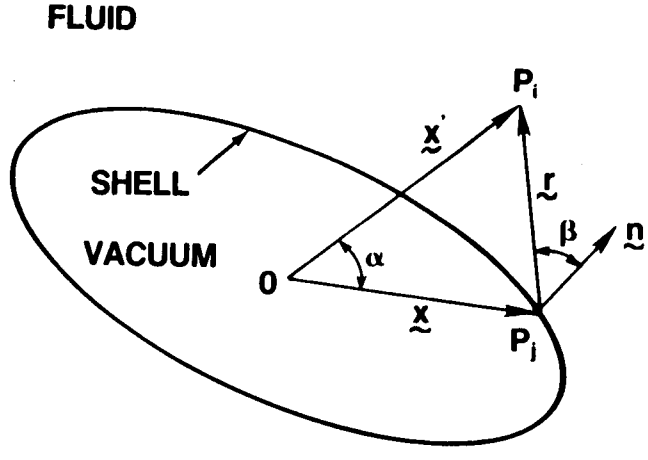

Fig. 1. Notation for Helmholtz integral equation.

where β is defined as the angle between the normal $\underline{n}$ and the vector $\underline{r}$, as shown in Fig. 1.

The substitution of Eqs. 11-13 into the surface equation (10) yields

$$p(\underline{x}')/2 - \int_S p(\underline{x})\ (e^{-ikr}/4\pi r)\ (ik + 1/r)\ \cos\beta\ dS$$

$$= i\omega\rho \int_S v_n(\underline{x})\ (e^{-ikr}/4\pi r)dS. \tag{14}$$

This integral equation relates the fluid pressure p and normal velocity v_n on S. If Eq. 14 is discretized for numerical computation (the details of which were presented previously[9]), we obtain the matrix equation

$$Ep = Cv_n \tag{15}$$

on S. The dimensionality of this system (i.e., the dimension of vectors p and v_n) is f, the number of fluid DOF (the number of wet points on the surface S). Hence, the added mass matrix (the matrix which converts fluid acceleration to fluid force) is, in terms of the fluid DOF,

$$M_n = AE^{-1}C/i\omega, \tag{16}$$

where A is the diagonal fxf area matrix for the wet surface. As given above, M_n is full, symmetric, frequency-dependent, and complex. The low frequency (incompressible fluid) added mass matrix is obtained by evaluating M_n in the limit $\omega \to 0$. An inspection of the formulas[9] for the entries in the fluid matrices E and C reveals that, for small frequency, E is real and constant, and C is purely imaginary and proportional to ω. Thus, to compute M_n in Eq. 16, we consider only the real parts of E and $C/i\omega$ for small ω. With this interpretation, the added mass matrix M_n is now full, symmetric, real, and independent of frequency.

To relate the f normal DOF on the wet surface to the complete set of s independent structural DOF, we introduce a transformation matrix G, which is defined as the rectangular sxf matrix of direction cosines to transform a vector F_n of outward normal forces at the wet points to a vector F of forces at all points in the output coordinate systems selected by the user. Thus,[10]

$$F = GF_n, \quad v_n = G^T v, \quad \text{and} \quad a_n = G^T a, \tag{17}$$

where v and a are the velocity and acceleration vectors for the independent structural DOF, respectively, and the subscript n is used to denote the

outward normal components of these vectors. For time-harmonic analysis, $v = i\omega u$ and $a = i\omega v$. The transformation matrix G can then be used to transform the added mass matrix displayed in Eq. 17 from normal DOF to the independent structural DOF:

$$M_a = GAE^{-1}(C/i\omega)G^T. \tag{18}$$

Here again, we consider only the real parts of E and $C/i\omega$ for small ω. The matrix M_a given above is the boundary element equivalent of the finite element matrix of the same name defined following Eq. 9. M_a is real, symmetric, non-banded, and independent of frequency. (The symmetry of M_a, while not obvious from the above definition, follows by reciprocity arguments.)

We note that the coupling matrix L defined in Eq. 4 is the product of the transformation and area matrices G and A.

We clearly could have started with the Laplace, rather than the Helmholtz, integral equation and avoided the complex, frequency-dependent matrices.[11] We chose this approach since the four matrices G, A, E, and C needed to compute the added mass matrix M_a are readily available in NASTRAN form from the computer program called SURF, which is part of the NASHUA structural-acoustics package.

NASTRAN IMPLEMENTATIONS

Finite Element Approach

The finite element procedure used here to compute resonances of submerged shells is the symmetric potential formulation as shown in Eq. 5 except that, for incompressible fluids, the matrices Q and C are both zero. To solve this system with NASTRAN,[12] a finite element model is required for both the structure and a portion of the surrounding fluid. The model for the structure is constructed in the usual way. The model for the fluid domain is constructed using any of the general elastic elements which are geometrically compatible with the elements chosen for the structure. Thus, if the structure is modeled with QUAD4s, the fluid should be modeled with IHEX1s; if the structure is modeled with CONEAX elements, the fluid should be modeled with TRIAAX or TRAPAX elements.

Since the z component of displacement represents, by analogy (in both Cartesian and cylindrical coordinate systems), the scalar velocity potential q in Eq. 5, all other DOF at fluid mesh points are eliminated by single point constraints. The material properties are assigned to the fluid elements according to Eqs. 6 and 7a. If the fluid is considered to be of infinite extent, the finite element model of the fluid should be truncated not closer than one shell diameter away from the shell, where a pressure-release (q=0) boundary condition is imposed.

The coupling matrix L is entered as a symmetric "damping" matrix using NASTRAN's direct matrix input (DMIG) data cards. L has nonzero entries only at the intersections of matrix columns associated with interface fluid DOF with rows associated with the translational DOF of coincident structural points. Each nonzero entry of L is a component of the outwardly-directed area vector, which is a normal vector whose magnitude is equal to the area assigned to a wet point. The resulting system is solved using NASTRAN's direct complex eigenvalue analysis (Rigid Format 7) because of the presence of the coupling matrix in the "damping" matrix. (However, since there is no actual damping, all the natural frequencies are real.)

Since both structural and fluid DOF are included in the finite element model, the interpretation of tabular output is aided if only the structural DOF are printed and the printing of the fluid unknowns is suppressed.

Boundary Element Approach

The boundary element generation of the added mass matrix is implemented using the fluid matrix generation capability available in the NASHUA processor called SURF.[9] For each unique set of symmetry constraints, the procedure involves two steps, the first of which is identical to the first step of a NASHUA structural-acoustic analysis. In general, this step is a NASTRAN analysis whose primary purpose is to generate an OUTPUT2 file containing geometric information and the definition of the wet surface of the structure. The second step (described here for the first time for added mass matrix generation) involves the sequential execution of SURF (which generates the matrices G, A, E, and C appearing in Eq. 18) followed by NASTRAN for the real eigenvalue analysis. For completeness, we describe both steps in the boundary element approach to compute submerged resonances.

The first step is a modified NASTRAN direct frequency response analysis in which the structure is defined and an outwardly-directed static unit pressure load applied to the wet faces of all elements in contact with the exterior fluid. This load, which is invoked using the case control card LOAD, is used to generate areas and normals. In addition, the following DMAP Alter is inserted into the Executive Control Deck:

```
ALTER     1 $ NASHUA STEP 1, COSMIC 1988 RF8 (REVISED 12/14/87)
ALTER     21,21 $ REPLACE GP3
GP3       GEOM3,EQEXIN,GEOM2/SLT,GPTT/S,N,NOGRAV/NEVER=1 $ SLT
ALTER     117,117 $ REPLACE FRRD
SSG1      SLT,BGPDT,CSTM,SIL,EST,MPT,GPTT,EDT,MGG,CASECC,DIT/
          PG/LUSET/NSKIP $ PG
SSG2      USET,GM,YS,KFS,GO,DM,PG/QR,PO,PS,PL $ PL
OUTPUT2   BGPDT,EQEXIN,USET,PG,PL $
OUTPUT2   CSTM,ECT,, $
OUTPUT2   ,,,, //-9 $
EXIT      $
ENDALTER $
```

The UT1 file created by OUTPUT2 must be saved after the NASTRAN execution.

The second step in this procedure consists of the sequential execution of the NASHUA processor SURF followed by NASTRAN. SURF reads the UT1 file generated in Step 1 and generates the matrices G, A, E, and C appearing in Eq. 18. These matrices are written in NASTRAN's INPUTT2 format. Since SURF generate's the frequency-dependent fluid matrices E and C for compressible fluids, a small (but nonzero) frequency must be specified as input for the generation of these matrices. The nondimensional frequency ka = 0.01 is a reasonable choice, where a is a typical length (e.g., radius) of the structure. Following SURF, a modified NASTRAN real eigenvalue (Rigid Format 3) analysis is performed. The following DMAP Alter is included in this run:

```
ALTER    1 $ ADDED MASS MATRIX, COSMIC 1988 RF3 (REVISED 12/22/88)
ALTER    3 $
INPUTT2  /G,A,CT,E,DAT $ READ FLUID MATRICES FROM SURF
ALTER    69 $ BEFORE READ
PARAML   DAT//*DMI*/1/2/FREQ $ GET FREQ FROM DAT
PARAMR   //*COMPLEX*//FREQ/0./FREQC $ FREQ+I*0
PARAMR   //*MPYC*////W/FREQC/(6.283185,0.) $ OMEGA
PARAMR   //*MPC*////IW/W/(0.,1.) $ I*OMEGA
PARAMR   //*DIVC*////IWI/(1.0,0.0)/iw $ 1/IW
DIAGONAL A/PVECF/*COLUMN*/0. $ FLUID SET VECTOR OF 1'S
DIAGONAL KAA/PVECA/*COLUMN*/0. $ A-SET VECTOR OF 1'S
ADD      CT,/CTIW/IWI $ CT/IW
PARTN    CTIW,PVECF,/,,CTIWR,/1/1 $ EXTRACT REAL PART OF CT/IW
PARTN    E,PVECF,/,,ER,/1/1 $ EXTRACT REAL PART OF E
TRNSP    G/GT $
TRNSP    CTIWR/CIW $
SOLVE    ER,CIW/EICIW $
MPYAD    A,EICIW,/AEICIW/1 $ REAL NONSYM ADDED MASS (FLUID DOF)
PARTN    AEICIW,PVECF,/,,MADDF,/1/1///6 $ REAL SYM ADDED MASS (F-DOF)
MPY3     GT,MADDF,/MADDS $ REAL SYM ADDED MASS (STRUCTURAL DOF)
ADD      MAA,MADDS/MSUM $ STRUCTURAL + ADDED MASS
EQUIV    MSUM,MAA $ REPLACE MAA WITH SUM
ENDALTER $
```

This Alter combines the input matrices G, A, E, and C to form the added mass matrix M_a according to Eq. 18 and replaces the structural mass matrix M with the sum $M + M_a$. To assure compatibility with the frequency used in SURF, the frequency is passed from SURF to NASTRAN for use in this Alter. The real parts of the complex matrices E and $C^T/i\omega$ are extracted as soon as possible in the Alter so that less expensive real arithmetic can be performed as much as possible. (Real parts of matrices can be extracted by executing a dummy PARTN module to redefine a complex matrix as real. The same trick can also be used to declare as symmetric a symmetric matrix which NASTRAN thinks is nonsymmetric.)

The use of checkpoint may optionally link the two steps in this procedure. However, in any case, the user must ensure that NASTRAN's internal grid point sequence (as generated by the BANDIT module) is the same in both

steps. Otherwise, the sequence used for the generation of the SURF matrices would not agree with that used when the matrices are combined in the second step.

NUMERICAL EXAMPLE

We illustrate these procedures by computing, using both finite element and boundary element techniques, the fluid-loaded resonances of a submerged cylindrical shell with flat end closures. The particular problem solved has the following characteristics:

$a = 5$ m	mean shell radius
$L = 60$ m	shell length
$h = 0.05$ m	shell thickness (shell and end plate)
$E = 1.96 \times 10^{11}$ N/m^2	Young's modulus
$\nu = 0.3$	Poisson's ratio
$\rho_s = 7900$ kg/m^3	shell density
$\rho = 1000$ kg/m^3	fluid density
$c = 1500$ m/sec	fluid speed of sound

For the finite element model of both structure and fluid, a half-length model was prepared using axisymmetric elements (the conical shell CONEAX for the shell and the triangular ring TRIAAX for the fluid), as shown in Fig. 2. The structural model consisted of 25 elements over the half-length and four elements on the end plate. The outer boundary of the fluid model was located about 16 meters from the axis of the shell. Symmetry conditions were imposed at the mid-length, thus restricting the available modes to those symmetric with respect to the mid-length. The NASTRAN bulk data for this model were generated automatically by a special purpose fluid-structure data generator called SFG written by Richard J. Kazden of the David Taylor Research Center.

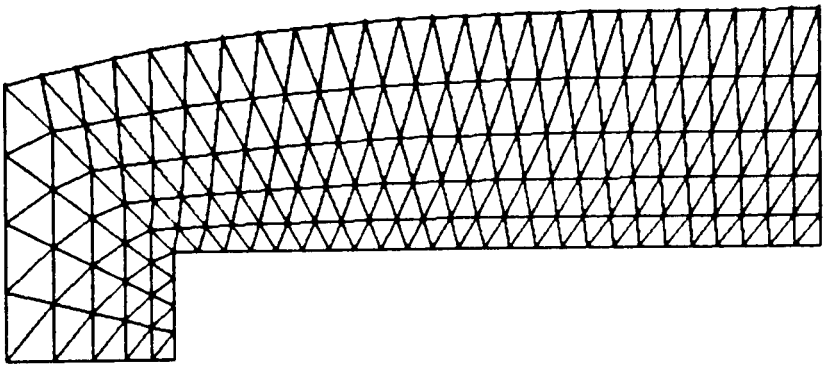

Fig. 2. Axisymmetric finite element model of structure and fluid.

For the analysis with added mass effects generated by boundary elements, a general shell model of the structure was prepared using NASTRAN's four-node isoparametric membrane/bending quadrilateral plate element QUAD4. A quarter model was prepared (half the length and half the circumference) using 25 elements longitudinally, 12 elements circumferentially, and four elements radially on the end plate, as shown in Fig. 3. Symmetry was imposed at both planes of geometric symmetry. Since all fluid effects were computed by the NASHUA processor SURF, no fluid mesh was required.

Four analyses were performed for this problem:

1 - conical shell model, in-vacuo, circumferential harmonic $n \leq 5$, 715 DOF,

2 - QUAD4 model, in-vacuo, 2093 DOF,

3 - conical shell model, fluid-loaded, finite element added mass effects, $n \leq 5$, 1465 DOF, and

4 - QUAD4 model, fluid-loaded, boundary element added mass effects, 2093 DOF (matrices not banded).

The first 21 natural frequencies and mode shapes were found among those which have circumferential index $n \leq 5$ and are symmetric with respect to the mid-length plane. The results of these calculations are shown in the table on the next page. The second column in the table (Harm. n) denotes the circumferential harmonic index, the number of full waves around the circumference. (For the end plate, n thus denotes the number of nodal diameters.) The third column (Shell m) denotes the number of longitudinal half waves. The fourth column (Plate m) denotes the number of nodal circles (plus one) in the end plate. The next two columns of the table list the in-vacuo natural frequencies (in Hz.) of the cylindrical shell for both the conical shell and QUAD4 models. The next two columns of the table list the

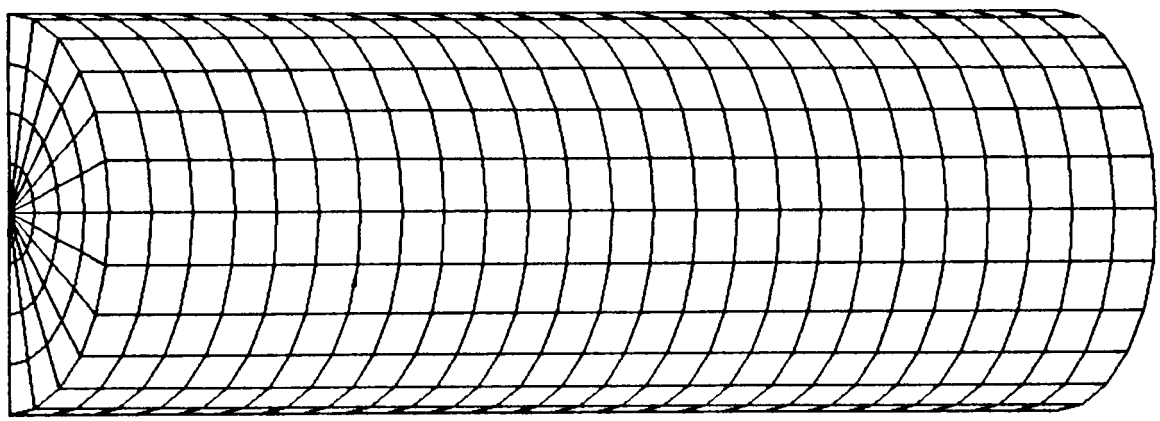

Fig. 3. QUAD4 finite element model of cylindrical shell.

Table. In-Vacuo and Fluid-Loaded Natural Frequencies of Cylindrical Shell with Flat End Plates

	Mode			Frequency (Hz)				
	Harm.	Shell	Plate	CONEAX	QUAD4	CONEAX subm.	QUAD4 subm.	Approx.
No.	n	m	m	in-vacuo	in-vacuo	(F.E. mass)	(B.E. mass)	Theory
1	1	0		0	0	0	0	0
2	2	1		2.72	2.72	1.13	1.13	1.11
3	3	1		3.84	3.90	1.79	1.81	1.77
4	0		1	4.27	4.22	1.63	1.44	1.38
5	4	1		7.04	7.19	3.61	3.67	3.57
6	4	3		9.29	9.34	4.81	4.82	4.70
7	1		1	9.53	9.20	4.44	4.26	4.22
8	3	3		10.4	10.4	4.94	4.93	4.82
9	5	1		11.3	11.6	6.31	6.38	6.18
10	5	3		12.2	12.4	6.83	6.86	6.67
11	1	3		13.4	13.3	7.04	6.88	
12	2		1	15.6	15.1	8.31	8.02	
13	5	5		15.8	15.9	8.99	8.88	8.65
14	0		2	15.9	16.4	8.66	8.40	
15	4	5		17.0	16.9	8.94	8.85	8.66
16	2	3	3	18.6	18.5	8.05	8.07	7.75
17	3		1	22.7	22.4	13.2	13.0	
18	5	7		22.9	22.8	13.2	12.9	12.6
19	3	5		24.5	24.1	11.9	11.9	11.5
20	1		2	26.6	27.2	15.4	15.5	
21	4	7		28.4	28.2	15.3	15.1	14.7

fluid-loaded (fully submerged) resonances of the shell using both models. The added mass effects were computed for the conical shell and QUAD4 models using, respectively, the finite element and boundary element techniques described above.

The last column of the table lists approximate theoretical predictions for the fluid-loaded resonances. These values are computed in the following way. In general, since frequency is inversely proportional to the square root of mass, the ratio of submerged to in-vacuo resonant frequencies for a structure is

$$f_{wet}/f_{dry} = (1 + M_a/M)^{-1/2}, \tag{19}$$

where M_a and M are the added mass and structural mass, respectively. For both plates and cylindrical shells, this ratio of added to structural mass can be written in the form[13,14]

$$M_a/M = \alpha(\rho/\rho_s)(a/h), \tag{20}$$

where α is a dimensionless parameter which depends on the boundary conditions, modal wavenumbers, and, for the case of a cylinder, the length-to-radius ratio. For a finite length, simply supported cylindrical shell, α can be approximated for the lobar ($n > 1$) modes as[13]

$$\alpha = n^2/((n^2 + 1)(n^2 + (m\pi a/L)^2)^{1/2}). \tag{21}$$

For a clamped circular plate,[14] $\alpha = 0.6689$ for the (0,1) mode and 0.3087 for the (1,1) mode, where the two mode numbers denote, respectively, the number of nodal diameters and the number of nodal circles plus one. Since the conditions under which these relations apply are approximately satisfied with our example, we include their predictions in the table for reference. The ratio, Eq. 19, is applied in the table to the average of the two in-vacuo predictions.

As indicated in the table, most of these 21 modes are either predominantly shell modes or predominantly end plate modes. For one mode (16), the shell and end plate are both active participants in the modal behavior (although with varying levels of relative participation, depending on the model and whether there was fluid loading).

The results in the table show generally very good agreement between the predictions of the two approaches, both in-vacuo and fluid-loaded, even for circumferential harmonics 4 and 5. For these two harmonics, the QUAD4 mesh has only six and 4.8 elements per wavelength in the circumferential direction, respectively, but still does surprisingly well. The two numerical approaches show agreement to within about 2% for all the fluid-loaded modes which exhibit predominantly shell behavior. The two fluid-loaded predictions for the end plate modes all agree to within about 4%, with the exception of Mode 4, the fundamental drum head mode of the plate, where the difference is about 12%. In view of the similarity of the boundary element prediction to the approximate theoretical prediction, the boundary element result is probably the better of the two numerical predictions, perhaps indicating that the finite element mesh used (Fig. 2) needs to be extended a little farther out at the end of the structure.

DISCUSSION

From the results presented in the preceding section, we conclude that both the finite element and boundary element procedures are capable of computing accurate added mass effects due to fluid loading on fully submerged structures. Of the two approaches, the boundary element procedure is the easier to use, since it is highly automated and does not require the generation of a fluid mesh. Even general purpose automatic mesh generators cannot completely solve the fluid meshing issue, since they cannot generate

the fluid-structure interface condition, which requires direct matrix input of surface areas. On the other hand, the finite element procedure is somewhat more general, since it can also treat structures which are near a free surface (or other boundary) or are partially submerged.[5] The boundary element procedure used is applicable only to deeply submerged structures (i.e., structures far enough from a fluid boundary so that the boundary can be ignored).

For structures similar to the cylindrical shell considered here, the finite element procedure is also computationally less expensive than the boundary element procedure. This difference is due primarily to the exploitation by the finite element method of the banded matrices which occur with long, slender structures. Consider, for example, the QUAD4 model of the cylindrical shell shown in Fig. 3. The in-vacuo model had 2093 independent DOF with an average matrix wavefront of 79. When the (boundary element) added mass matrix was combined with the structural mass matrix, the average wavefront increased about five-fold to 394. With the eigensolution time proportional to the product of the order of the matrix and the square of the wavefront, the solution time for the submerged case increases by a factor of about 25. On the other hand, a finite element model of a portion of the surrounding fluid would typically double both the matrix order and the matrix wavefront (compared to the in-vacuo case) since each structural grid point (with six DOF) would require about six fluid grid points (each with one DOF) to be added to the model. Such a model would therefore cost only about eight times as much to run as the "dry" model. The trade-off between the finite element and boundary element procedures for solving the underwater vibration problem thus reduces to a trade-off of engineering time with computer time.

It is concluded therefore that both the finite element and boundary element procedures are capable of computing the fluid loading effects needed for underwater resonance calculations and that the more elegant boundary element approach is easier to use but may be more expensive computationally.

REFERENCES

1. T.L. Geers, "Residual Potential and Approximate Methods for Three-Dimensional Fluid-Structure Interaction Problems," J. Acoust. Soc. Amer. 49, 1505-1510 (1971).

2. G.C. Everstine, "Structural-Acoustic Finite Element Analysis, with Application to Scattering," in Proc. 6th Invitational Symposium on the Unification of Finite Elements, Finite Differences, and Calculus of Variations, edited by H. Kardestuncer (Univ. of Connecticut, Storrs, Connecticut, 1982), pp. 101-122.

3. G.C. Everstine, "A Symmetric Potential Formulation for Fluid-Structure Interaction," J. Sound and Vibration 79, 157-160 (1981).

4. G.C. Everstine, "Structural Analogies for Scalar Field Problems," Int. J. Num. Meth. in Engrg. 17, 471-476 (1981).

5. M.S. Marcus, "A Finite-Element Method Applied to the Vibration of Submerged Plates," J. Ship Research 22, 94-99 (1978).

6. A.J. Kalinowski and C.W. Nebelung, "Media-Structure Interaction Computations Employing Frequency-Dependent Mesh Sizes with the Finite Element Method," The Shock and Vibration Bulletin 51, Part 1, 173-193 (1981).

7. L.H. Chen and D.G. Schweikert, "Sound Radiation from an Arbitrary Body," J. Acoust. Soc. Amer. 35, 1626-1632 (1963).

8. D.T. Wilton, "Acoustic Radiation and Scattering From Elastic Structures," Int. J. Num. Meth. in Engrg. 13, 123-138 (1978).

9. G.C. Everstine, F.M. Henderson, E.A. Schroeder, and R.R. Lipman, "A General Low Frequency Acoustic Radiation Capability for NASTRAN," in Fourteenth NASTRAN Users' Colloquium (National Aeronautics and Space Administration, Washington, DC, 1986), NASA CP-2419, pp. 293-310.

10. G.C. Everstine, F.M. Henderson, and L.S. Schuetz, "Coupled NASTRAN/ Boundary Element Formulation for Acoustic Scattering," in Fifteenth NASTRAN Users' Colloquium (National Aeronautics and Space Administration, Washington, DC, 1987), NASA CP-2481, pp. 250-265.

11. J.A. DeRuntz and T.L. Geers, "Added Mass Computation by the Boundary Element Method," Int. J. Num. Meth. in Engrg. 12, 531-549 (1978).

12. "NASTRAN User's Manual," NASA SP-222(08), Computer Software Management and Information Center (COSMIC), University of Georgia, Athens, Georgia (1986).

13. M.C. Junger and D. Feit, Sound, Structures, and Their Interaction (The MIT Press, Cambridge, Massachusetts, 1986), 2nd ed.

14. R.D. Blevins, Formulas for Natural Frequency and Mode Shape (Van Nostrand Reinhold Company, New York, 1979).